International Journal of Control, Automation, and Systems (2010) 8(5):1091-1099 http://www.springer.com/12555
DOI 10.1007/s12555-010-0518-8

Development of Unmanned Aerial Vehicle (UAV) System with Waypoint Tracking and Vision-based Reconnaissance

Dong-in Han, Jong-hun Kim, Chan-oh Min, Sung-jin Jo, Jeong-ho Kim, and Dae-woo Lee*

Abstract: This paper introduces the developed UAV system for low cost operation and an EOS (Electro Optical System) laboratory. This paper highlights an autonomous navigation system based on microcontrollers that can track a target using images, take three-dimensional measurements of the target, and acquire high quality images. The hardware system and an algorithm for the EOS verify the performance of the image tracking system and 3-D measurement of the target's position. 3-D position estimations for the target are solved using the mathematical relationship between the UAV and target. Although an on-board EOS can make errors in 3-D measurement, the proposed approach shows improved accuracy and confidence for 3-D target tracking using a postprocessing method.

Keywords: Electro-optical system, flight control system, Kalman filter, image tracking, microprocessor, monocular vision, unmanned aerial vehicle.

1. INTRODUCTION

Recently, the importance of unmanned systems has increased in many industries due to the advancement of automation technology. The military has always sought ways to reduce casualties; in response, the aerospace industry has made rapid progress in the development of UAVs. The processor of a UAV flight control system must be compact, highly controllable, and inexpensive. Recently, processors such as the PC/104 or DSP have dominated the UAV market. The PC/104 provides performance comparable to that of a desktop personal computer, but is bigger and heavier than a microprocessor. On the other hand, DSP can overcome these shortcomings, but is still expensive to be included with the development kit.

Using an EOS, 3-D positioning of the target is calculated using the mathematical relationship between the UAV and targets. To obtain an accurate measurement between the UAV and target, an INS (Inertial Navigation System) and GPS (Global Positioning System) system are being studied. Also, a machine vision system has recently been researched. A vision system on a UAV is necessary to acquire information on the target, and to operate missions such as surveillance of mountains or oceans. For civil use, observering fire in the mountains has been researched [1], and searching algorithms to track persons or cars in urban areas has been studied [2]. Guidance and contol using machine vision has been applied to UAV to structure monitoring [3].

In the fields of ground vehicles and robots, machine vision has been studied to measure the distance between obstacles. In [4], a vision system was used in an avoidance system. An omnidirectional mirror was equipped on a robot, and the distance and depth from the obstacle was computed using this vision system.

This paper introduces the developed FCC (Flight Control Computer) that uses only an 8-bit microprocessor, which is inexpensive and easily manufactured, to carry out the basic mission of the UAV. In adition, a 3-D measurement algorithm for EOS is developed and applied to a hardware system. To obtain the 3-D position of a target, the dynamics is derived using the relationship among the coordinates of the UAV, target, and reference.

2. HARDWARE CONFIGURATION

2.1. Flight control system

The flight control system consists of a main controller, GPS, AHRS (Attitude Heading Reference System), actuator, communication system, power supply, and GCS (Ground Control System). The main processor performes the calculations and controls the plane for autonomous flight, so it must be stable and reliable.

The AHRS gives the plane's attitude and position information to the subprocessor which calculates the algorithm to control the surfaces of the plane directly via the actuator. Also, the states of the plane can be observed at the ground station via the communication system, which can be used to transmit the control command from the ground station to the UAV when it is needed. Fig. 1 shows UAV system configuration.

Manuscript received August 3, 2009; revised March 4, 2010; accepted March 30, 2010. Recommended by Editorial Board member Hyo-Choong Bang under the direction of Editor Jae-Bok Song. This research was financially supported by the Ministry of Education, Science Technology (MEST) and Korea Institute for Advancement of Technology (KIAT) through the Human Resource Training Project for Regional Innovation.

Dong-in Han, Jong-hun Kim, Chan-oh Min, Sung-jin Jo, Jeong-ho Kim, and Dae-woo Lee are with Pusan National University, Jangjeon 2-dong, Geumjeong-gu, Pusan 609-735, Korea (e-mails: {sunnyban, kjh1053, mingoon01, bestjsj, kimsmap, baenggi}@pusan.ac.kr).
* Corresponding author.

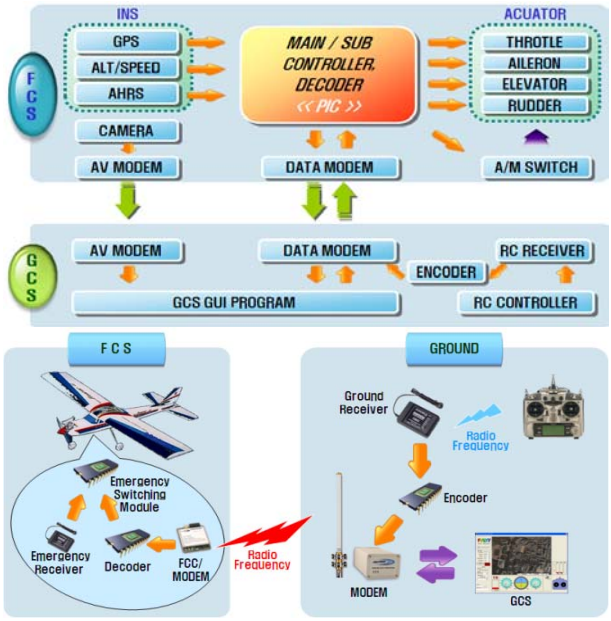

Fig. 1. UAV system configuration.

2.2. Main and subprocessor

An 8-bit PIC18F8722 main processor and 8-bit PIC16F873A subprocessor are used in the UAV (Microchip Technology, Inc.) as shown in Fig. 2.

The PIC18F8722 has a 131 Kbyte program memory and 4 Kbyte data memory. Through 16 10-bit ADC channels, it can measure altitude. The air speed sensor can detect the battery residual quantity by changing the voltage to a digital value. The PWM (Pulse Width Modulation) value of each control surface is captured using three 16-bit timers. Also, through the two channels

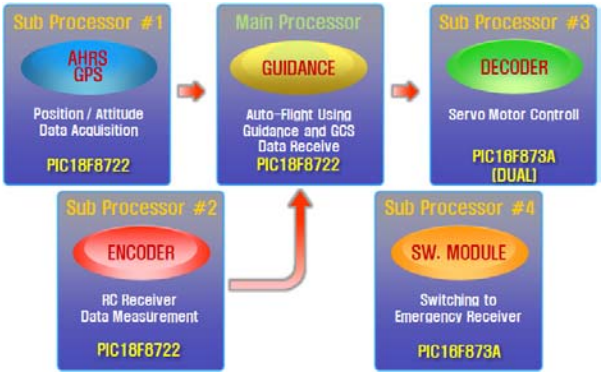

Fig. 2. Processor configuration.

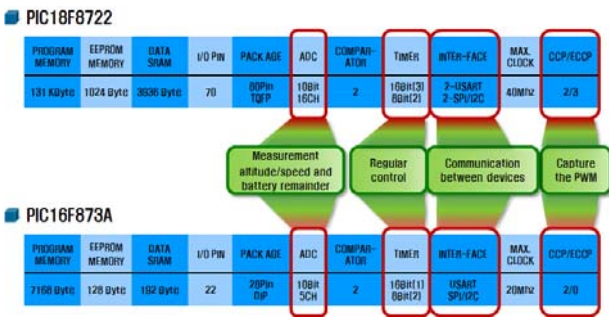

Fig. 3. PIC 18/16 specifications and functions.

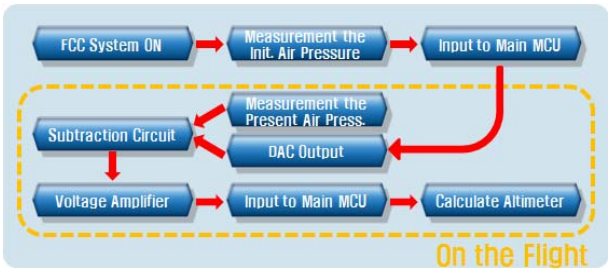

Fig. 4. Flowchart of altitude measurement.

of the UART (Universal Asynchronous Transmitter) function, all data can be transmitted and received between devices. Fig. 3. shows specifications and functions of PIC processor.

2.3. Sensors

The GPS receiver used in this study(NovAtel Inc.) has comparatively high performance and accuracy by altitude range in 18 km and speed range in nearly 1850 km/h. This GPS receiver has also data output mode using NMEA protocol, which includes the GSA protocol for position information and the GGA protocol for satellite information.

The altimeter aims the vertical position in flight, and corrects the error of the altitude data of the GPS. An aneroid method is used to measure atmospheric pressure and convert it to altitude. Voltage displayed according to altitude is amplified about the centuple using an OP-AMP as shown in Fig. 4.

The speedometer displays the flight speed and is used for position control calculations. The total pressure and static pressure are measured using a pressure sensor and pitot tube. Then, the dynamic pressure is calculated to provide the speed of aircraft. Usually, two pressure sensors are used: one measures the total pressure connecting the pitot tube, and the other measures the static pressure. An inertial measurement unit (IMU) is used to obtain data on the position of the UAV. The obtained data are three-axis angular acceleration and velocity components, so they must be integrated and be passed through filtering process to correct the values. However, it is difficult to obtain detailed data and the data require a complicated filtering process. Therefore, AHRS is used to obtain attitude data (roll, pitch, yaw angle component, and three-axis velocity and acceleration components).

An RF data modem is used for communication to receive and confirm all sensor data of the UAV during flight. The antenna in the modem greatly affects the communication equipment. It is important to choose high gain value antenna, because a gain of antenna causes much effect in activity area of UAV. A directional antenna has a high gain value, but the UAV uses a non-directional dipole antenna due to the UAV's wide active area.

2.4. Subprocessor module

2.4.1 Sensor data receiving processor

The sensor data of the GPS and AHRS are integrated

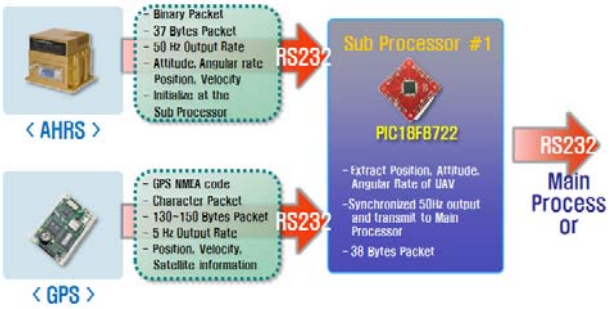

Fig. 5. Subprocessor for receiving sensor data.

into one packet and transmitted to the main processor as shown in Fig. 5. Because the PIC processor has an 8-bit calculation system and has only two of the UART serial communication channels, this packet-switched communication system decreases the amount of GPA and AHRS data at 2600 bytes/s to two-thirds of its size, thereby reducing the load on the main processor for communication with GCS.

2.4.2 Control signal encoder

This system transforms an analog signal from the R/C controller into a digital signal and transmits data to the FCC through the modem. Generally, the control range is 1-2 km using RC(Radio Control), but the encoder communicates with the modem to transmit data, so the control range expands significantly. The encoder is located at the ground and transforms all channels of a PWM analog signal into a 16-bit digital signal using the CCP function of the PIC processor. Fig. 6 represents a schematic composition of encorder system.

The internal clock of the PIC is 5 MHz and the prescaler rate of the CCP interrupt used to capture a PWM signal is 1:1; therefore, the PWM value is 7500 when the servomotor is in the central position as shown in Table 1.

$$Command = 0.0015(\text{sec}) / \frac{1}{5,000,000} = 7,500 \qquad (1)$$

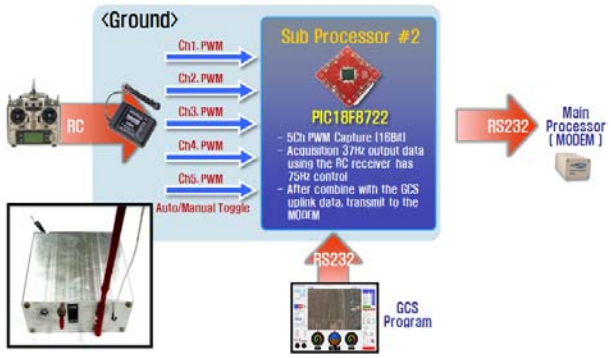

Fig. 6. Encoder for control signal.

Table 1. The revolution of PWM capture.

Servo Position	Right 45 deg	Center	Left 45 deg
PWM (ms)	1.0	1.5	2.0
Command	5,000	7,500	10,000

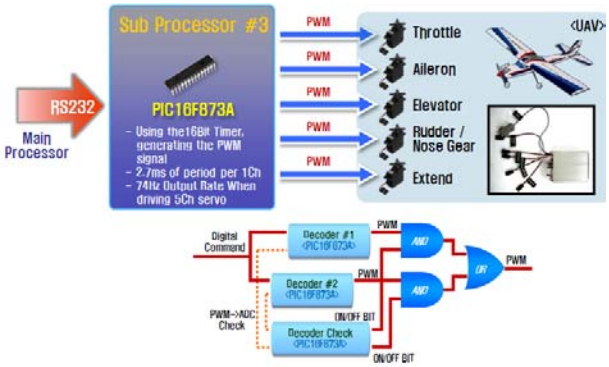

Fig. 7. Decoder for control signal.

2.4.3 Control signal decoder

The control values calculated in the guidance algorithm and the controller of the FCC are transmitted to the control signal decoder, and this subprocessor generates PWM signals because the main controller must carry out many internal data calculations and interrupts of the A/D conversion. Therefore, the main controller dose not generates the PWM signals but digital values, and the decoder receives these values and generates the PWM signals. The decoder receives only a few data and only uses the timer interrupt, so the PIC16F873 is used for the decoder. The decoder uses the same clock and pre-scaler rate as the encoder. Fig. 7 represents a schematic composition of decorder system.

2.5. Peripheral system configuration

2.5.1 Power supply

Usually the engine of an aircraft runs on fuel, but the processors, sensors, and devices in the aircraft systems are supplied with battery-powered electricity. The servomotor (actuator) has low power consumption but requires a sudden high output, so it uses a power supply separate from the power supply of the main processor and uses a dc-to-dc converter for safety.

The measured power consumption was about 0.7 A, excluding the power consumed by the servomotors; thus, the aircraft can operate for about 3 hr using a 11.1 V 2100 mAh battery. Fig. 8 shows a division of the power source.

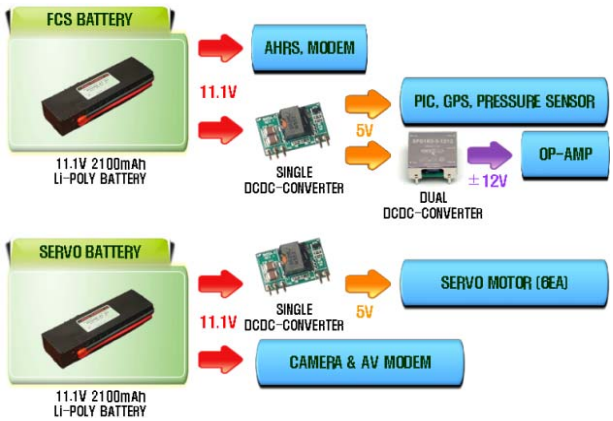

Fig. 8. Division of the power source.

2.5.2 GCS GUI program

The GCS transfers data with the FCC in the aircraft to obtain information on the status of mission operations, the attitude of the vehicle, the flight trajectory, and the stored data. This system is programmed in Visual C++. based RS232 communication receives information on the operational status of the vehicle, and transmits control signals for the mission. Fig. 9. depicts the GCS program.

On the ground, two GCSs operate to command and acquire information. One is the data GCS, which shows the state of the UAV and commands the UAV to fly to a waypoint or achieve the mission. The other is the vision GCS. Figs. 10 and 11 show the operational system between the UAV and GCS, and GCS pack for PNUAV, respectively.

Fig. 9. GCS program.

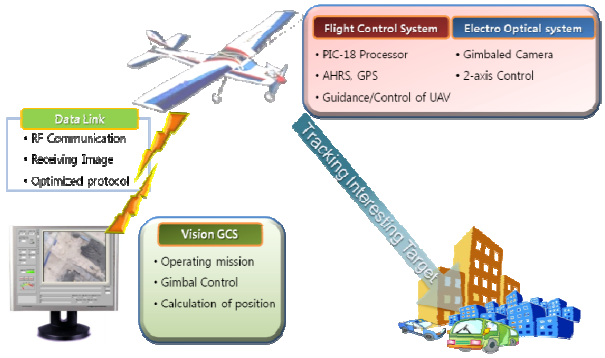

Fig. 10. System description of PNUAV.

Fig. 11. Ground control system pack.

Table 2. Plane and engine specification for flight test.

Wingspan	2,050 mm	Fuselage	1,635 mm
Wing Area	79.5 m^2	Engine	OSFS91SIII
EmptyWeight	3,300 g	Displacement	14.95 cc

Fig. 12. Plane and engine for flight test.

2.5.3 Flight test vehicle

Commercially available RC planes are pre-verified for flight performance, so the verification of flight stability for safety is not necessary. Nevertheless, UAVs have various payloads such as the autonomous navigation system and the electro-optical system. Thus, the vehicle is remodeled to enlarge the space available for a payload, and to reinforce the vehicle for greater impact at touchdown due to the weight increase. The design of this vehicle is changed but it is based on the Super Frontier Senior-60 model for loading payloads. Also, the engine is also changed to the OS Engine FS-120 model as shown in Table 2 and Fig. 12.

2.5.4 Electro-optical system

The EOS of a PNUAV consists of a transmission system, gimbal controller, and image acquisition system. The gimbal controller provides the control input for pan and tilt movements. Camera zoom and focus are also controlled by the gimbal controller. Fig. 13 shows the gimbal operating process. Fig. 14 shows the camera gimbal we developed for this study.

The vision GCS is built using LabVIEW. This shows the image from the PNUAV, and has a command window where the user can input the angle of the gimbal's pan and tilt, as well as other control inputs.

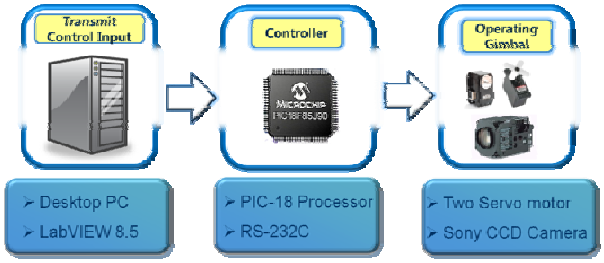

Fig. 13. Gimbal operating process.

Fig. 14. Camera gimbal and controller.

Command from the user input is transmitted to the gimbal controller through data GCS. The GCS sends control inputs to move the EOS, and to maneuver the UAV.

Because of the characteristics of LabVIEW, the block diagram of the vision GSC is represented in two parts. One part is the code for communication. In this block, information on the PNUAV's states is classified for 3-D measurement, and the 3-D measurement algorithm is initiated and processed. The other part is image processing. A Kalman filter is used during this process for image tracking.

3. GUIDANCE ALGORITHM

3.1. Guidance and controller

The UAV has various waypoints from which it can obtain images and identify a target, so the correct and accurate passing of the waypoint is a very important performance index for UAV operation. Point navigation guidance is used in the flight test.[5] The guidance logic is based on the difference between the line-of-sight angle, which is measured from the reference axis to the waypoint, and the UAV's heading angle, which is set as an error equal to zero. In straight and level flight, the angle of the velocity vector and the LOS angle are used for lateralal-directional control. The longitudinal guidance uses proportional control based on the difference between the present altitude and the target altitude. Fig. 15 depicts the lateral-directional and longitudinal guidance.

When only the P controller is used, the overshoot increases. On the other hand, if the PID controller is used, the steady state error can be reduced. The integral gain have less influence on flight performance and computation load is added to the main processor. For this reason, the PD controller is used. The PD controller uses the derivative term of the angle, so it makes different to the weight of control. That is, the effect of the fluxion is small when the flight is straight. However, if the LOS angle grows, the control value will increase, and then the UAV will show a fast response. Figs. 16 and 17 represent the block diagram of control system and subsystem function.

$$\phi_{cmd} = k_1 \cdot [LOS - \psi_{body}] + k_2 \cdot \frac{d[LOS - \psi_{body}]}{dt}, \qquad (2)$$

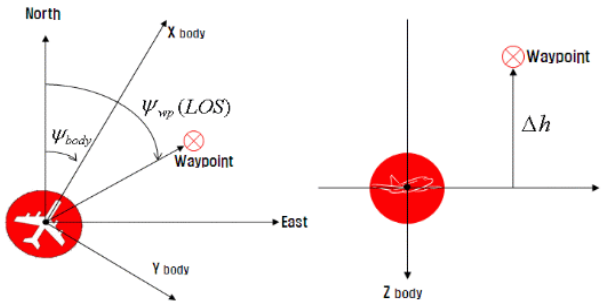

Fig. 15. Lateral-directional and longitudinal guidance.

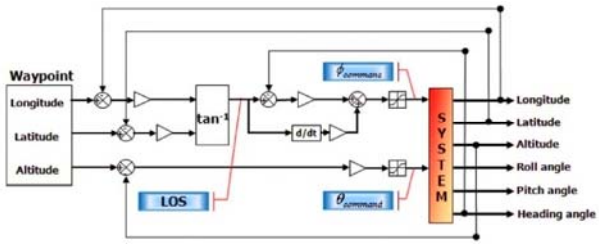

Fig. 16. Design PD controller.

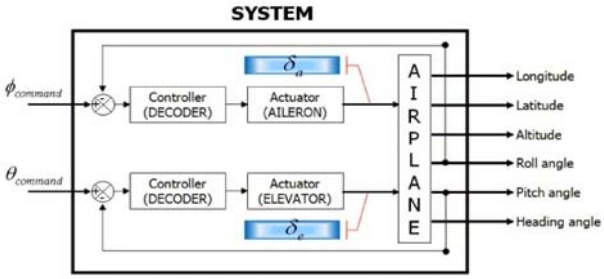

Fig. 17. Subsystem function.

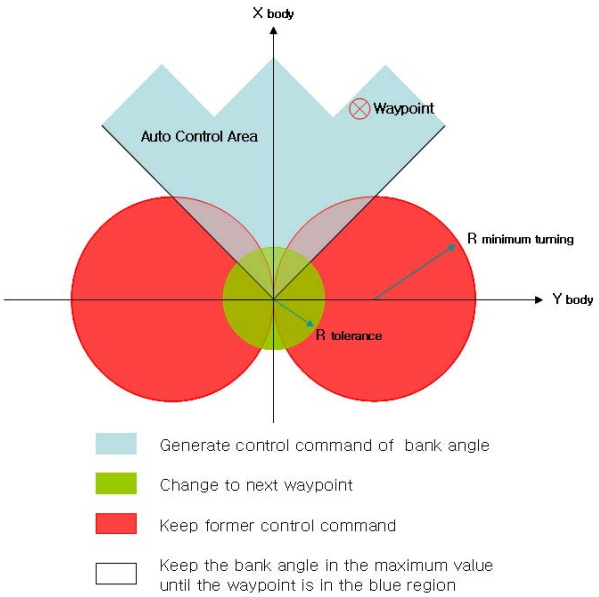

Fig. 18. Control range at body axis.

$$\theta_{cmd} = k_3 \cdot \Delta h. \qquad (3)$$

The ranges of ϕ_{cmd} and θ_{cmd} are

$$-\frac{\pi}{4} \le \phi_{cmd} \le \frac{\pi}{4}, \quad -\frac{\pi}{6} \le \theta_{cmd} \le \frac{\pi}{6}. \qquad (4)$$

When the UAV passes a waypoint without converging, the waypoint is in the minimum turning range. The UAV will fly, turning many times. Therefore, in this case, the UAV must escape the minimum range to follow the former control command. Fig. 18 shows the geometric relations of UAV flight control range and the waypoint.

3.2. Fail safe system

Sometimes various outbreak situations happen during UAV operations, so countermeasures are needed. The

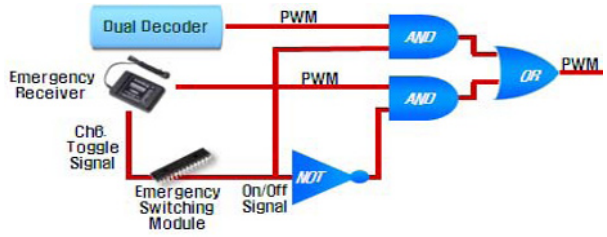

Fig. 19. Emergency receiver system.

UAV's survival is of primary importance. In flights under automatic control, if there is a problem, the solution would be to return to the base position or to convert immediately to manual flight. This system has four flight modes for fail safety:

1) Automatic mode: A mode that controls the UAV by FCC according to the guidance algorithm.

2) Manual mode: A mode that controls the UAV to put commands directly to the decoder at the ground through the modem.

3) Return mode: A mode that commands the UAV to return to the established take-off point due to breakdown of various types of communication equipment failure, for communication blackouts of more than 3 seconds, for unusual states of flight, or at the command of the pilot or GCS controller.

4) Perfection manual mode: A mode that controls the UAV directly through the RC receiver on board the UAV without going through the modem. This mode is safer than other modes because of receiving no effects of other equipment.

Emergency receiver system should be added to the FCC for fail safety as shown in Fig. 19. First, the RC receiver is installed in the encoder. This device converts the control signal to the PWM and sends the signal via the decoder. The emergency RC receiver, in addition to UAV to compose perfection manual mode can control through RC without going through modem using this, greatened greatly stability. Fig. 19 shows the logic diagram of the return mode.

4. 3-D MEASUREMENT ALGORITHM

Fig. 20 shows the dynamic relationship between the UAV, EOS, and GCS. The coordinate system of the

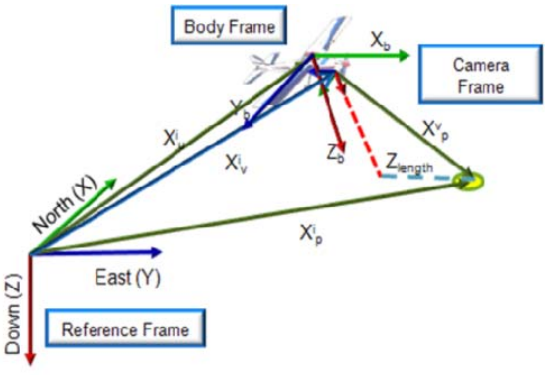

Fig. 20. 3-D coordinate system.

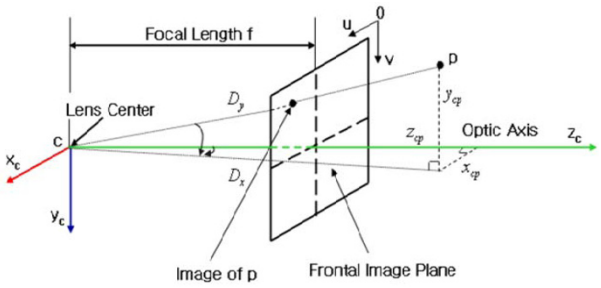

Fig. 21. Coordinates of camera.

camera uses to derive the 3-D position from the 2-D image is shown in Fig. 21 [6].

The 3-D position of the target is calculated from a monocular image as shown in (5) and (6):

$$x = f\frac{x}{z}, \tag{5}$$

$$y = f\frac{y}{z}, \tag{6}$$

where f is the focal length, (x,y) is the position in the image, and (X,Y,Z) is the position in the real spacer. If the position along the Z-axis is known, the 3-D information can be determined. However, the 3-D information obtained from (5) and (6) is the result with respect to the camera frame. To transfer the coordinates from the camera to the reference frame, the attitudes of the camera and UAV are necessary. The attitude of a UAV with respect to a fixed body coordinate is known as an onboard AHRS. The attitude of the camera is defined in Fig. 22. The gimbal of the camera rotates along x,y and is called ϕ, ψ, respectively.

To obtain the position along Z, we assume that the target is on a flat plane (zero altitude), and the attitudes of the UAV and camera can be measured. Using a directional vector from the camera axes, the attitudes of the UAV and camera are obtained. A linear equation in 3-D is made from a unit directional vector from the camera to the target at zero altitude. The distance along Z-axis is derived from a linear equation. Equations (7) and (8) represent a unit directional vector and the distance along Z-axis, respectively [8]:

$$\vec{l} = (T_V^i)^{-1}(T_c^v)^{-1}[0 \quad 0 \quad 1]^T, \tag{7}$$

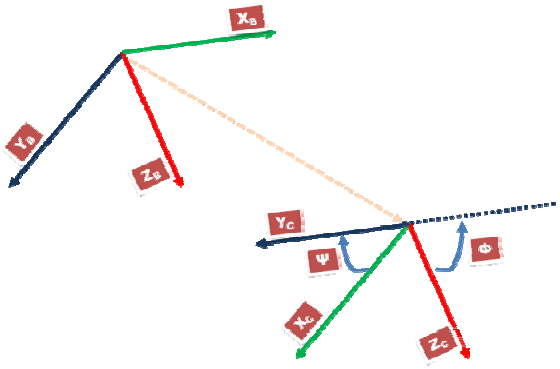

Fig. 22. Coordinate relations between UAV and camera.

$$\|\vec{m}\| = \sqrt{(\frac{l_1 Z_V^i}{l_3})^2 + (\frac{l_2 Z_V^i}{l_3})^2 + (Z_V^i)^2}, \quad (8)$$

where $\vec{l}$ is the unit directional vector between the camera and the target, T_V^i is the Euler transformation matrix of the UAV attitude with respect to the reference, and T_c^V is the Euler transformation matrix of the camera attitude with respect to the UAV. Z_V^i is the altitude of the UAV with respect to the reference frame.

5. AUTONOMOUS FLIGHT TEST

5.1. Ground test

Autonomous tests must be carried out on the ground to obtain the desired results before the algorithm is applied to the UAV. Using the RC car, a test of the point navigation guidance algorithm was carried out at Pusan National University. The test equipment consisted of the car, RF-modem, GPS receiver, GCS program, and decoder processor.

To edit the guidance algorithm quickly, the test car have a GPS receiver, modem, and decoder processor, excluding the main processor. As shown in Fig. 23, the GPS position data are transmitted to the ground computer via the modem, and the computer calculates and re-transmits the result of the guidance algorithm to the car. Then, the decoder processor controlls the actuator directly.

As shown in Fig. 24, we can verify that the test car converges to the waypoints well.

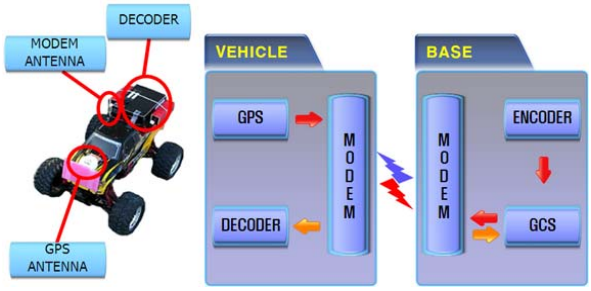

Fig. 23. Ground test system.

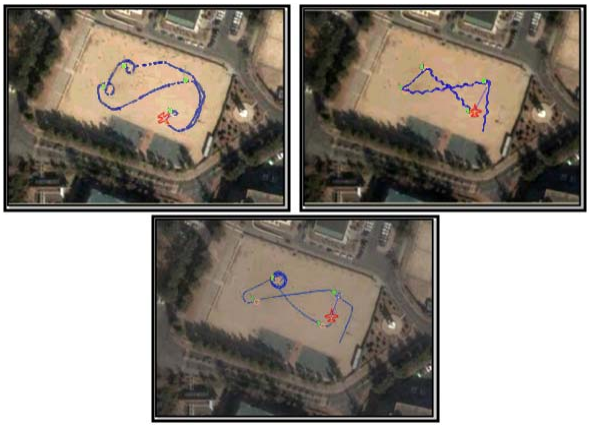

Fig. 24. Ground test result and gain tuning.

5.2. Flight test

The flight test was based on the results of the ground test and was carried out in two stages. In the first stage, flight safety was proven by manual flight using the encoder and decoder. The manual flight resulted in slight damage to landing gear caused by the payload. However, there were no flight problems, and the data was correctly transmitted, received, encoded, and decoded.

In the second stage, the UAV was successfully carried out an autonomous waypointing flight, and verified what can apply real basically mission. The flight test gave good results. However, the limit of roll and pitch angle was so large that it forced slow turning and a circular flight. To set the lower limit and tune the gain, the flight performance was improved. In Fig. 25, the lower-left paths were the result of the UAV passing the five-waypoint continuously, and the right path was the result of circular flight to one waypoint as the center.

Fig. 26 shows the result of a flight in wind. In this case, errors are caused by the influence of crosswind. However, in Fig. 27, the bank angle as the control input converges

Fig. 25. Flight test results.

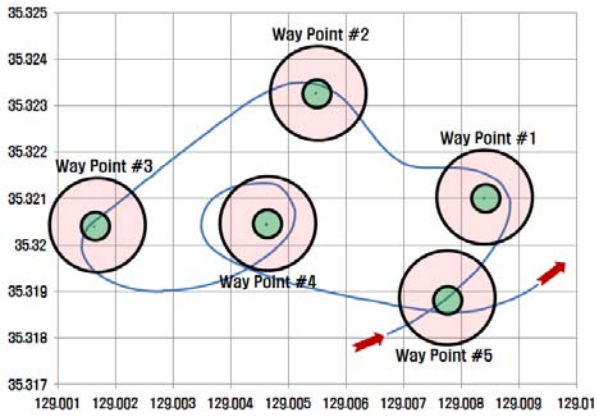

Fig. 26. Autonomous flight path.

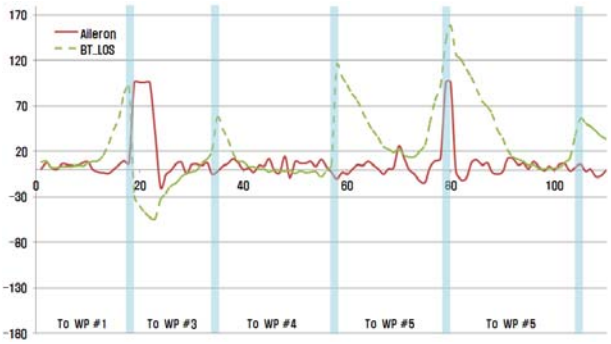

Fig. 27. LOS and aileron command.

Table 3. Minimum distance from target.

Waypoint	1	2	3	4	5
Error distance(m)	39	23	9	43	29

to zero, and the UAV is controlled to the waypoint. This result proves that the proposed flight control system using the 8-bit processor has stability and can carry out basic missions without any problem. The error distances to the waypoints are shown in Table 3.

5.3. 3-D measurement test

In this study, 3-D positioning of the target is solved using mathematical relationships between the UAV and the targets. The electro-optical system on the UAV can make errors in 3-D measurement.

When a UAV operates on a surveillance mission, the results of 3-D measurement are scattered as shown in Fig. 28. In this example, the average of the results is (8.51 m, 63.80 m), and the position of the real target is (11.87 m, 61.06 m). The distance error from the real target is 4.3 m. This error is small with respect to the altitude of the UAV. However, the distribution of points on the graph has low confidence. To increase the confidence of the result, postprocessing is necessary.

In this study, we adopted a simple method of postprocessing. After 2-D vectors of the results are converted to magnitude, the points in bound $\pm 1\sigma$ are selected The

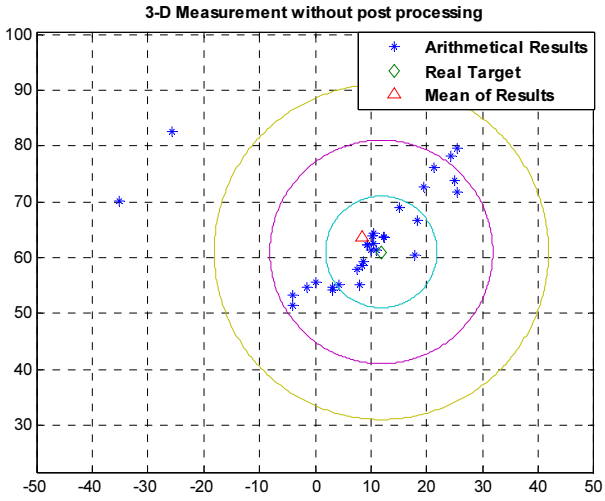

Fig. 28. 3-D measurement without postprocessing.

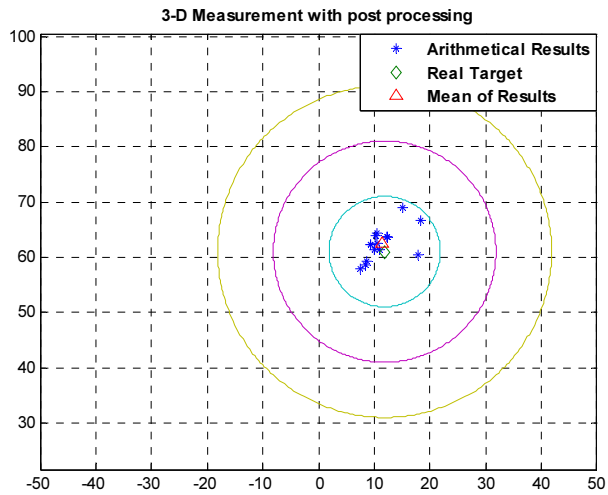

Fig. 29. 3-D measurement postprocessing.

results after postprocessing have greater confidence as shown in Fig. 29. The average of the points is (11.47 m, 61.61 m), and distance error from the real target is 1.6 m. Therefore, we can verify that postprocessing algorithm results in greater accuracy and confidence.

6. CONCLUSION

This paper presents the development of overall system from the flight control computer and guidance/control algorithm to the electro-optical target tracking system. Moreover, the performance of waypoing for a developed UAV is verifies by practical flight experiment. These results may be considered to get high evaluation because the FCC with low-cost processors only yields good results. The developed laboratory-level onboard EOS can also measure the 3-D position of a target from acquired monocular images. The tracking results of EOS can be improved by using a 3-D measurement postprocessing algorithm. To track a target, the EOS requires precise information about the target. Postprocessing, using the average and the distribution of the measurements, can give more precise target information.

It is apparent that this UAV system can be used for observation of forest fires or the seaside to open new vistas in the design of civilian UAV systems.

REFERENCES

[1] L. Merino, A. Ollero, J. Ferruz, J. R. Martinez-de-Dios, and B. Arrue, "Motion analysis and Geolocation for aerial monitoring in the COMETS multi-UAV system," *Proc. ICAR 2003*, Coimbra, Portugal, 2003.

[2] K. Nordberg, P. Doherty, G. Farneback, P.-E. Forssen, G. Granlund, A. Moe, and J. Wiklund, "Vision for a UAV helicopter" *Proc. of IROS'02, Workshop on Aerial Robotics*, October 2002.

[3] N. Metni and T. Hamel, "Visual tracking control of aerial robotic systems with adaptive depth estimation," *International Journal of Control, Automation, and Systems*, vol. 5, no. 1, pp. 51-60, February

2007.
[4] S. Yi, B. Choi, and N. Ahuja, "Real-time omni-directional distance measurement with active panoramic vision," *International Journal of Control, Automation, and Systems*, vol. 5, no. 2, pp. 184-191, April 2007.
[5] S.-C. Han, H. Bang, and C.-S. Yoo, "Proportional navigation-based collision avoidance for UAVs," *International Journal of Control, Automation, and Systems*, vol. 7, no. 4, pp. 553-565, 2009.
[6] J.-H. Kim, D.-W. Lee, and K.-R. Cho, "Vision-based indoor object tracking using mean-shift algorithm," *Journal of Control, Automation, and Systems Engineering* (in Korean), vol. 12, no. 8, pp. 746-751, Aug 2006.
[7] M. V. Cook, *Flight Dynamics Principles*, John Wiley & Sons Inc., New York, 1997.
[8] C. O. Min, M. J. Kim, J. W. Shin, D. Y. An, S. P. Yang, W. M. Jang, and D. I. Han, "The development of flight control system for unmanned aerial vehicle," *Pusan National University 3C Project*, 2007-3CPJT-7, 2007.
[9] C. H. Heo, M. S. Roh, D. W. Lee, and K. R. Cho, "Flight performance test and analysis of the super frontier-60," *Proc. of CASS*, Korea, pp. 313-317, 2006.

Dong-in Han received his B.S. degree in Aerospace Engineering from Pusan National University in 2010. His research interests include UAV systems, guidance, and control.

Jong-hun Kim received his B.S. degree in Aerospace Engineering from Pusan National University in 2005. His research interests include using optical tracking, head-eye tracking, and trajectory control.

Chan-oh Min received his M.S. degree in Aerospace Engineering from Pusan National University in 2010. His research interests include re-entry vehicle trajectory control.

Sung-jin Jo received his B.S. degree in Aerospace Engineering from Pusan National University in 2009. His research interests include lunar module guidance and control.

Jeong-ho Kim received his B.S. degree in Aerospace Engineering from Pusan National University in 2008. His research interests include vision based tracking, head/eye tracker system.

Dae-woo Lee received his Ph.D. degree in Aerospace Engineering from Pusan National University in 2001. His research interests include UAV flight control system, image tracking, space flight dynamics, and guidance and control for re-entry vehicle.